

## Electron mobility in very low density GaN/AlGaNGaN heterostructures

M. J. Manfra, K. W. Baldwin, A. M. Sergent, R. J. Molnar, and J. Caissie

Citation: *Appl. Phys. Lett.* **85**, 1722 (2004); doi: 10.1063/1.1784887

View online: <http://dx.doi.org/10.1063/1.1784887>

View Table of Contents: <http://apl.aip.org/resource/1/APPLAB/v85/i10>

Published by the [American Institute of Physics](#).

---

### Related Articles

Laterally aligned quantum rings: From one-dimensional chains to two-dimensional arrays  
*Appl. Phys. Lett.* **100**, 203117 (2012)

Partially filled intermediate band of Cr-doped GaN films  
*Appl. Phys. Lett.* **100**, 202101 (2012)

Ultrafast carrier response of Br<sup>+</sup>-irradiated In<sub>0.53</sub>Ga<sub>0.47</sub>As excited at telecommunication wavelengths  
*J. Appl. Phys.* **111**, 093721 (2012)

GaN epitaxy on Cu(110) by metal organic chemical vapor deposition  
*Appl. Phys. Lett.* **100**, 192110 (2012)

A liftoff process of GaN layers and devices through nanoporous transformation  
*Appl. Phys. Lett.* **100**, 181908 (2012)

---

### Additional information on *Appl. Phys. Lett.*

Journal Homepage: <http://apl.aip.org/>

Journal Information: [http://apl.aip.org/about/about\\_the\\_journal](http://apl.aip.org/about/about_the_journal)

Top downloads: [http://apl.aip.org/features/most\\_downloaded](http://apl.aip.org/features/most_downloaded)

Information for Authors: <http://apl.aip.org/authors>

## ADVERTISEMENT



**Goodfellow**  
metals • ceramics • polymers • composites  
70,000 products  
450 different materials  
**small quantities fast**

[www.goodfellowusa.com](http://www.goodfellowusa.com)

## Electron mobility in very low density GaN/AlGaN/GaN heterostructures

M. J. Manfra,<sup>a)</sup> K. W. Baldwin, and A. M. Sergent  
Bell Laboratories, Lucent Technologies, 700 Mountain Avenue, Murray Hill, New Jersey 07974

R. J. Molnar and J. Caissie  
Massachusetts Institute of Technology, Lincoln Laboratory, 244 Wood Street, Lexington,  
Massachusetts 02420-9108

(Received 19 December 2003; accepted 22 June 2004)

We report on the transport properties of a tunable two-dimensional electron gas (2DEG) confined at the lower interface of a GaN/Al<sub>0.06</sub>Ga<sub>0.94</sub>N/GaN heterostructure grown by plasma-assisted molecular beam epitaxy on semi-insulating GaN templates prepared by hydride vapor phase epitaxy. Using an insulated gate Hall bar structure, the electron density is continuously tuned from  $\sim 2 \times 10^{12}$  down to  $1.5 \times 10^{11}$  cm<sup>-2</sup>. At  $T=300$  mK, the 2DEG displays a maximum mobility of 80 000 cm<sup>2</sup>/V s at a sheet density of  $1.75 \times 10^{12}$  cm<sup>-2</sup>. At low densities, the mobility exhibits a power law dependence on density  $-\mu \sim n_e^\alpha$ , with  $\alpha \sim 1.0$ , over the range of  $2 \times 10^{11}$ – $1 \times 10^{12}$  cm<sup>-2</sup>. In this density regime, the mobility is no longer limited by alloy scattering and long-range Coulomb scattering dominates. We discuss the dominant scattering mechanisms that presently limit low temperature mobility at electron densities below  $1 \times 10^{12}$  cm<sup>-2</sup>. © 2004 American Institute of Physics. [DOI: 10.1063/1.1784887]

The quality of the two-dimensional electron gas (2DEG) realized in the AlGaN/GaN system has improved dramatically in recent years.<sup>1–4</sup> Nevertheless, many of the basic electron scattering processes are still poorly understood, especially in the low-density regime ( $n_e < 2.0 \times 10^{12}$  cm<sup>-2</sup>) where few experiments have been performed. It is now well established<sup>1,3,5</sup> that alloy scattering and interface roughness limit the low temperature mobility for densities above  $\sim 2 \times 10^{12}$  cm<sup>-2</sup>, producing a characteristic decrease in mobility for increasing density. At low densities, however, the electron wave function samples the heterointerface less and also penetrates less into the AlGaN barrier such that interface roughness and alloy scattering become less significant. In this regime, Coulomb scattering from unintentional background impurities, charged threading dislocations, and charged surface states is expected to limit mobility. In the low-density regime, the functional dependence of mobility on density for AlGaN/GaN heterostructures has not been experimentally determined and is a topic of theoretical discussion.<sup>5–9</sup> It will, of course, depend on the nature and location of the Coulomb scattering sites. The functional dependence of low temperature mobility on density is thus a sensitive probe of the dominant scattering mechanisms.

In this letter we detail our studies of the dependence of low temperature mobility on carrier density in the very low-density regime. Using an insulated gate Hall bar structure we have succeeded in producing a 2DEG with densities as low as  $1.5 \times 10^{11}$  cm<sup>-2</sup>, thereby reducing the measurable density by a factor of 10 over previously reported results<sup>1,2</sup>.

The 2DEGs used in this study were grown by nitrogen plasma-assisted molecular beam epitaxy (MBE) on thick GaN templates prepared by hydride vapor phase epitaxy (HVPE) on (0001) sapphire substrates. The HVPE GaN template is 40  $\mu$ m thick and is known to have an approximate threading dislocation density of  $10^8$  cm<sup>-2</sup>. The HVPE GaN has been compensated with Zn at a level of  $\sim 10^{17}$  cm<sup>-3</sup> to

suppress any residual conductivity that may obscure observation of the 2DEG properties at very low sheet charge densities. The MBE epitaxial layer consists of a 1.5  $\mu$ m GaN buffer followed by a 16 nm Al<sub>0.06</sub>Ga<sub>0.94</sub>N undoped barrier layer that is capped with a 3 nm GaN layer. Insulated gate Hall bars are then fabricated. Mesas of 100 nm height are defined with a chlorine-based dry etch. Ohmic contacts consist of a Ti/Al/Ni/Au metal stack that is thermally annealed at 800°C for 30 s. The Hall bar is not intentionally aligned along any particular crystallographic axis. The Hall bar is 100  $\mu$ m wide by 2.0 mm long. Fourteen voltage probes are placed symmetrically along the device. After Ohmic contact definition, 100 nm of SiO<sub>2</sub> is deposited on the device. Finally, 10 nm of Ni and 100 nm of Au are deposited over the SiO<sub>2</sub> along the Hall bar forming an insulated gate structure. The device and epilayer structure is shown schematically in Fig. 1. At  $T=0.3$  K, the gate leakage is  $\leq 10^{-12}$  A over a voltage range  $\pm 4$  V. The gate voltage dependence of  $n_e$  at  $T=0.3$  K is displayed in Fig. 2(a). The 2DEG density at each gate voltage is determined from the periodicity of the

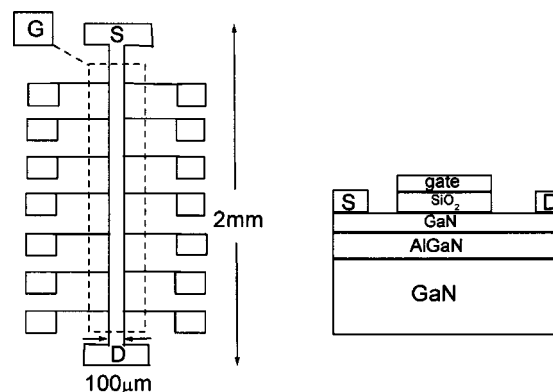


FIG. 1. Schematic diagram of the epilayer and the device used in this study. The Hall bar is 2 mm long by 100  $\mu$ m wide. The distance between adjacent voltage probes is 300  $\mu$ m. The SiO<sub>2</sub> layer between the epilayer surface and the gate metal is 100 nm.

<sup>a)</sup>Electronic mail: manfra@lucent.com

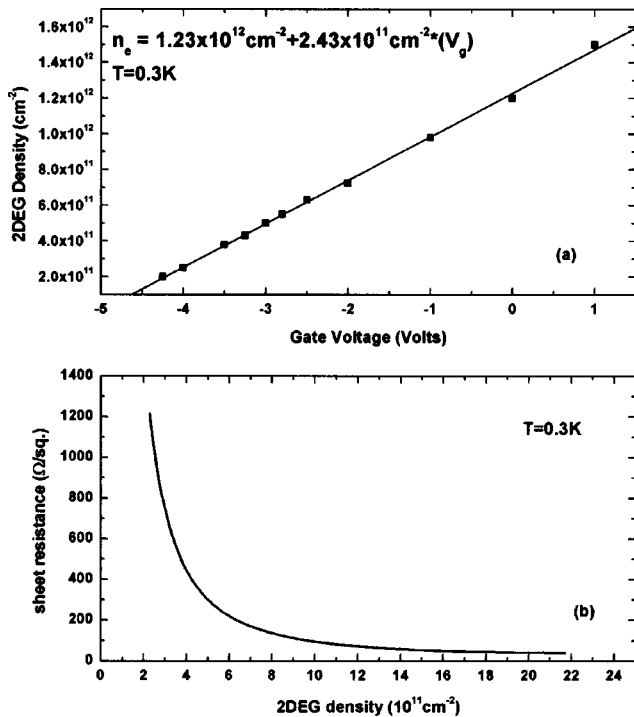


FIG. 2. (a) Measured 2DEG density at  $T=0.3$  K as a function of gate voltage  $V_g$  between 1 and  $-4.25$  V. In this regime,  $n_s$  vs  $V_g$  is linear and well approximated by  $n_e = 1.23 \times 10^{12} + 2.42 \times 10^{11} \text{ cm}^{-2} * V_g$ . (b) 2DEG sheet resistance as a function of electron density at  $T=0.3$  K.

Shubnikov–de Haas (SdH) oscillations. In all cases, the longitudinal magnetoresistance,  $R_{xx}$ , goes to zero at the integer quantum Hall states at high magnetic field, confirming that only one conduction channel is active. As can be seen, the 2DEG density is a linear function of the gate voltage and our device is behaving as a simple parallel plate capacitor. Figure 2(b) displays the sheet resistance of our device as a function of 2DEG density at  $T=0.3$  K.

The density dependence of mobility at  $T=0.3$  K is shown on a log–log plot in Fig. 3. The mobility exhibits three distinct regions. At low electron density, the mobility rapidly increases for increasing density. The mobility peaks

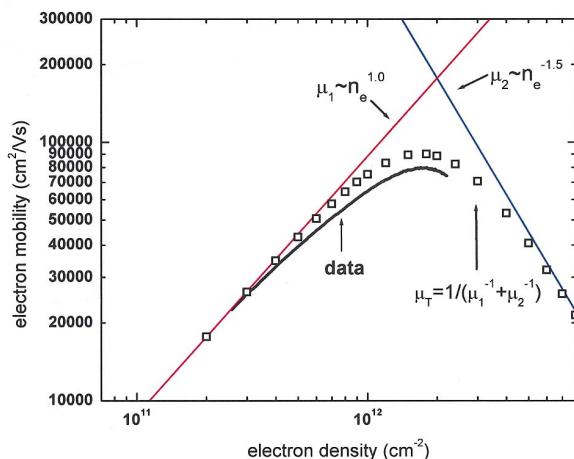


FIG. 3. (Color) Mobility at  $T=0.3$  K solid black curve is the experimentally measured mobility as a function of 2DEG density from  $\sim 2 \times 10^{11}$  to  $\sim 2 \times 10^{12} \text{ cm}^{-2}$ . For comparison, the red line displays the function  $\mu_1 \sim n_e^{1.0}$  at low density and the blue line represents  $\mu_2 \sim n_e^{-1.5}$  in the high-density regime. The open black squares are calculated from  $\mu_T = 1/(\mu_1^{-1} + \mu_2^{-1})$ .

at  $80\,000 \text{ cm}^2/\text{V s}$  at a density of  $\sim 1.7 \times 10^{12} \text{ cm}^{-2}$ . Above a density of  $\sim 2 \times 10^{12} \text{ cm}^{-2}$  the mobility decreases for further increases of density. The decrease in mobility with increasing density above  $2 \times 10^{12} \text{ cm}^{-2}$  is known to be a consequence of increased alloy and interface roughness scattering.<sup>1,3,5</sup>

The rise in mobility with increasing density for densities below  $1 \times 10^{12} \text{ cm}^{-2}$  is the central finding of this work. In AlGaIn/GaN heterostructures at low temperatures it is believed that charged surface states (SS), unintentional background impurities (BI), and charged dislocations (CD) are the dominant sources of Coulomb scattering at low 2DEG density.<sup>8,9</sup> At  $T=0.3$  K phonons do not contribute significantly to scattering<sup>5</sup> and are neglected in this analysis. The inverse mobility can be expressed via Mathiessen's rule  $\mu^{-1} = \mu_{SS}^{-1} + \mu_{BI}^{-1} + \mu_{CD}^{-1} + \mu_{\text{alloy}}^{-1} + \mu_{\text{ir}}^{-1}$ . The interplay of these five mechanisms will determine the maximum achievable mobility and the exact functional dependence of mobility on  $n_e$  at low density. Empirically, we can approximate the observed dependence of mobility on density by assuming that mobility is governed by one power law in the low-density regime and that alloy scattering and interface roughness scattering result in another power law that is consistent with previous measurements in high-density regime<sup>3</sup>. The total mobility follows from Mathiessen's rule. This approach is applied in Fig. 3 using the functions  $\mu \sim n_e^{1.0}$  and  $\mu \sim n_e^{-1.5}$ . The total calculated mobility is shown as the open black squares. While this simple approximation does not capture all of the physics, it displays the required peak in mobility at  $n_e \sim 1.75 \times 10^{12} \text{ cm}^{-2}$ . At low densities, the mobility exhibits a power law dependence on density-  $\mu \sim n_e^\alpha$ , with  $\alpha \sim 1.0$ , over the range of  $2 \times 10^{11}$  to roughly  $1 \times 10^{12} \text{ cm}^{-2}$ . We note that we have now measured similar behavior in devices from three distinct wafers. The power law dependence in the low-density regime is indicative of mobility limited by Coulomb scattering from charged defects. This behavior is well known in the study of AlGaAs/GaAs structures<sup>10,11</sup> and can be qualitatively understood by the following simple model. The 2DEG mobility is most sensitive to scattering events that deflect charge significantly out of the current path. Since we are considering elastic scattering on the Fermi circle in two dimensions, the mobility is most affected by large angle scattering across the Fermi circle. The improved mobility at higher density can be attributed to the increase in the Fermi wave vector ( $k_F = \sqrt{2\pi n_e}$ ) that accompanies the rise in 2DEG density. For a given scattering wave vector  $q_s$  established by the spatial configuration of the Coulomb scattering sites, the angle through which the electron is scattered decreases with increasing  $k_F$ , and thus, the mobility is increased. Evidently, the peak in mobility of  $80\,000 \text{ cm}^2/\text{V s}$  at  $1.7 \times 10^{12} \text{ cm}^{-2}$  represents the point at which the improvement in mobility due to an increasing Fermi wave vector is counteracted by the increase in alloy scattering.

Jena *et al.*<sup>6</sup> evaluated the mobility limit due solely to charged dislocation scattering and predicted approximate  $n_e^{3/2}/N_{\text{dis}}$  dependence, where  $N_{\text{dis}}$  is the areal density of dislocations. Clearly the predicted  $\alpha$  differs from what is measured experimentally at lower densities. In fact, the calculated exponent  $\alpha \sim 3/2$  does depend on the ratio of  $q_{\text{TF}}$  to  $2k_F$  where  $q_{\text{TF}}$  is the Thomas–Fermi screening wave number.  $q_{\text{TF}} = 2/a_B$  where  $a_B$  is the effective Bohr radius in GaN. For the very low densities studied in our experiment, simple con-

siderations show that  $\alpha$  will be reduced to  $\alpha \sim 1.1$  if  $n_e \sim 5 \times 10^{11} \text{ cm}^{-2}$ , bringing  $\alpha$  closer to the experimentally measured value. In a later work Jena *et al.*<sup>9</sup> considered scattering from all five mechanisms and concluded that at low densities,  $n_e < 1 \times 10^{12} \text{ cm}^{-2}$ , dislocation scattering is the dominant scattering process for a dislocation density of  $\sim 5 \times 10^8 \text{ cm}^{-2}$  in which 35% of the dislocation trap sites are occupied. They predicted a maximum mobility of  $\sim 75\,000 \text{ cm}^2/\text{V s}$  at a density  $n_e \sim 1.5 \times 10^{12} \text{ cm}^{-2}$ —a result similar to our experimental finding. These calculations<sup>6,9</sup> and our observed power law dependence suggest that dislocation scattering dominates the low temperature mobility in our low-density samples. On the other hand, Hsu *et al.*<sup>5</sup> evaluated the mobility limit due to unintentional background impurities, charged surface state scattering, and alloy scattering *without* including the effects of dislocations. The explicit density dependence of mobility is not considered, but they do calculate that a maximum mobility of  $\sim 10^5 \text{ cm}^2/\text{V s}$  at  $n_e = 1.8 \times 10^{12} \text{ cm}^{-2}$  is possible for a heterostructure with a 15 nm  $\text{Al}_{0.07}\text{Ga}_{0.93}\text{N}$  barrier—a result that is also not significantly different from our measurement. The magnitude of the maximum calculated mobility will, of course, depend sensitively on the background impurity concentration chosen and the distance from the 2DEG to the surface used in the calculation. While the alloy composition and the surface to 2DEG distance is similar to ours, the authors used a residual  $n$ -type background doping of  $\sim 5 \times 10^{16} \text{ cm}^{-3}$  and a residual acceptor concentration of  $2.5 \times 10^{15} \text{ cm}^{-3}$ . Given our previously reported measurements<sup>3</sup> the chosen  $n$ -type impurity concentration may be overestimated by a factor of 100 and the agreement between experiment and theory may be fortuitous.

Figure 4 displays the longitudinal magnetoresistance,  $R_{xx}$ , measured at  $T=0.3 \text{ K}$  for several 2DEG densities in the same device in which the mobility study was performed. The lower density traces have been offset from zero for clarity. As the gate voltage is changed from  $-1$  to  $-3 \text{ V}$  the 2DEG density is reduced from  $9.8 \times 10^{11}$  to  $5 \times 10^{11} \text{ cm}^{-2}$ . Even at these low densities, the mobility is sufficiently high that well-developed integer quantum Hall states ( $R_{xx} \sim 0$ ) are evident. As can be seen, the longitudinal magnetoresistance evolves smoothly as the gate voltage tunes the sample to lower density. With this added control, we can now bring the low filling integer quantum Hall states into a readily accessible range of magnetic field. As shown in Fig. 4, the integer quantum Hall state near 10 T ( $R_{xx}=0$ ) can be progressively shifted from  $\nu=4$ , to  $\nu=3$ , and to  $\nu=2$ .

In summary, we have grown high mobility and low density AlGaIn/GaN heterostructures and fabricated an insulated gate Hall bar device that allows us to vary the 2DEG density by an order of magnitude while monitoring the mobility and the evolution of the magnetotransport. At low electron density the mobility obeys a power-law dependence ( $\mu \sim n_e^{1.0}$ ) and exhibits a peak mobility of  $80\,000 \text{ cm}^2/\text{V s}$  at  $n_e$

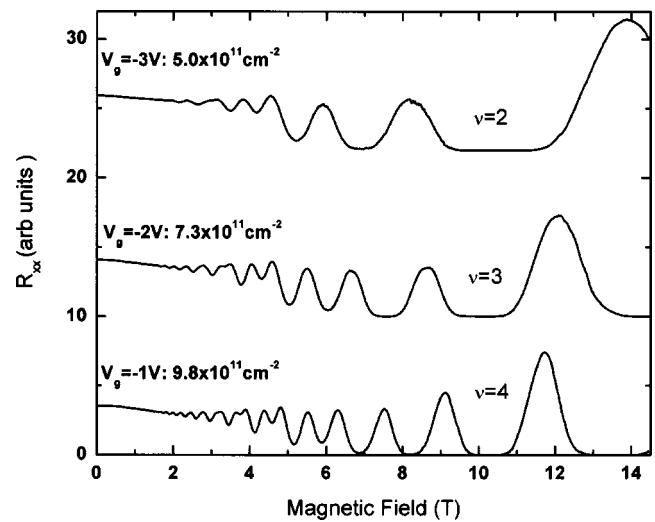


FIG. 4. Longitudinal magnetoresistance,  $R_{xx}$ , as a function of magnetic field at three different gate voltages. All data are taken at  $T=0.3 \text{ K}$ . The filling factor of several principle integer quantum Hall states is indicated. The two lower density traces are offset from zero for clarity.

$= 1.75 \times 10^{12} \text{ cm}^{-2}$ . The data are consistent with mobility limited by dislocation scattering at low electron density ( $n_e < 1.0 \times 10^{12} \text{ cm}^{-2}$ ).

One of the authors (M.J.M.) thanks S. Simon, H. L. Stormer, D. Jena, and L. N. Pfeiffer for many insightful conversations. The Lincoln Laboratory portion of this work was sponsored by the Office of Naval Research under Air Force Contract No. F19628-00-C-0002. Opinions, interpretations, conclusions and recommendations are those of the authors and not necessarily endorsed by the United States Air Force.

<sup>1</sup>I. P. Smorchkova, C. R. Elsass, J. P. Ibbetson, R. Ventry, B. Heying, P. Fini, E. Haus, S. P. DenBaars, J. S. Speck, and U. K. Mishra, *J. Appl. Phys.* **86**, 4520 (1999).

<sup>2</sup>E. Frayssinet, W. Knap, P. Lorenzini, N. Grandjean, J. Massies, C. Skierbiszewski, T. Suski, I. Grzegory, S. Porowski, G. Simin, X. Hu, M. Asif Khan, M. S. Shur, R. Gaska, and D. Maude, *Appl. Phys. Lett.* **77**, 2551 (2000).

<sup>3</sup>M. J. Manfra, L. N. Pfeiffer, K. W. West, H. L. Stormer, K. W. Baldwin, J. W. P. Hsu, D. V. Lang, and R. J. Molnar, *Appl. Phys. Lett.* **77**, 2888 (2000).

<sup>4</sup>M. J. Manfra, N. G. Weimann, J. W. P. Hsu, L. N. Pfeiffer, K. W. West, S. Syed, H. L. Stormer, W. Pan, D. V. Lang, S. N. G. Chu, G. Kowach, A. M. Sergent, J. Caissie, K. M. Molvar, L. J. Mahoney, and R. J. Molnar, *J. Appl. Phys.* **92**, 338 (2002).

<sup>5</sup>L. Hsu and W. Walukiewicz, *J. Appl. Phys.* **89**, 1783 (2001).

<sup>6</sup>D. Jena, A. C. Gossard, and U. K. Mishra, *Appl. Phys. Lett.* **76**, 1707 (2000).

<sup>7</sup>D. Jena and U. K. Mishra, *Appl. Phys. Lett.* **80**, 64 (2002).

<sup>8</sup>L. Hsu and W. Walukiewicz, *Appl. Phys. Lett.* **80**, 2508 (2002).

<sup>9</sup>D. Jena, I. Smorchkova, A. C. Gossard, and U. K. Mishra, *Phys. Status Solidi* **228**, 617 (2001).

<sup>10</sup>L. N. Pfeiffer, K. W. West, H. L. Stormer, and K. W. Baldwin, *Appl. Phys. Lett.* **55**, 1888 (1989).

<sup>11</sup>M. Shayegan, V. J. Goldman, M. Santos, T. Sajoto, L. Engel, and D. C. Tsui, *Appl. Phys. Lett.* **53**, 2080 (1988).